SCALING EFFECTS IN THE IMPACT RESISTANCE OF FLAT AND CYLINDRICAL SAMPLES FROM COMPOSITE MATERIALS

D.Sc. T.D. Karimbaev[1], A.Y. Ezhov[1], A.A. Chernyshov[1]

[1] Central Institute of Aviation Motors by P.I. Baranov, 111116, Aviamotornaya street 2, Moscow, Russia, Email: artem@ciam.ru, www.ciam.ru, tel: +7 (495) 362-49-72

Keywords: Scale factor, high-speed impact, fan case model, blade breakage, composite material

ABSTRACT

This study focuses on assessing the possibility of the possibility of using the test results when the blade of small-sized prototypes of fan cases breaks to predict the results of testing when the blade breaks on full-sized fan cases. Graphs of the dependence of various parameters for which the scale factors were successfully chosen, which allow to level the scale factor, were constructed.

1 INTRODUCTION

In practice, often, there are complex technical problems that are not amenable to direct analysis and experimental research. Such tasks are, for example,

- dynamic resistance of underground structures,
- a blow to nuclear fuel capsules,
- reactive impact of a nuclear power plant,
- protection against collisions of ships and others.

Although the problem of localization of a broken fan blade within the aircraft engine fan case is confirmed by experimental studies, the tests themselves are expensive, usually carried out at the latest stages of engine development, where the risk of getting a negative result should be practically zero.
The above and similar tasks from various fields of technology without involving small-scale models and without the use of similarity methods [1] can not be successfully solved. Obviously, in such cases, it is absolutely necessary to research and test constructively similar elements and small scale models of complex engineering structures and systems that present enormous financial and technical difficulties for theoretical analysis, numerical or full-scale experimental study. The risk of obtaining negative results in costly testing of full-size products is enormous, if the relevant studies and tests of constructive-like elements and small-scale models have not been carried out.

An analysis of foreign and domestic literature has shown that the problem of predicting the characteristics of resistance to impact of a product from the results of testing geometrically similar prototypes of small-scale size is certainly an actual and complex task that has not yet been adequately addressed. Many works are devoted to the development of methods for ensuring the reliability of statically loaded structures based on the use of scale factors. A sufficiently detailed survey of the investigations of this direction can be found in [2], [3]. A number of foreign articles (see, for example, [3]) describe the effect of a scale factor in a low-velocity impact of a coprode with a spherical tip over flat rectangular metal plates.

The purpose of this paper is to establish, on the basis of analytical studies, the parameters of geometric scaling in dynamic problems with high-speed impacts and to test the possibility of using them in samples of various shapes, in samples made from different materials, and under various dynamic impact conditions. The results of observations of the behavior of small-sized samples at high-speed impacts will allow predicting the consequences of interaction between the impactor and the proposed obstacle, significantly reducing the cost and simplifying the process of working out various design solutions.

2 MATHEMATICAL STATEMENT OF THE PROBLEM

A nonlinear problem of the penetration of a impactor into a deformable obstacle is considered. An elastic-deformable impactor of mass m in the form of a spherical body of radius r with a velocity $\partial s/\partial t = v_0$ normal to the surface of the obstacle at time t = 0 comes into contact with the resting obstacle. The displacements, deformations, stresses of the barrier at the initial moment are zero.

Further, the displacement s of the center of gravity of the impactor along the normal to the surface of the resisting (deformable) medium - the barrier is subject to the law

$$m\,\partial^2 s/\partial t^2 = F \tag{1}$$

Here m is the mass of the impactor, F is the resultant of the forces acting on the center of gravity of the impactor. The force F is the aggregate parameter due to the interaction of the energy of the impactor with the energy of the resisting medium. Changes in time of the contact surface of the impactor and the barrier, as well as the energy of penetration of the impactor into the obstacle, lead to nonlinearities similar to nonlinearities in the classical Hertz problem [4].

The barrier is a square laminated plate with two oppositely arranged fixed and free end surfaces. The impact is at the center of the square plate. To study the stress-strain state of the barrier, the equations of motion of the mechanics of a deformed solid are used

$$\sigma_{ij,j} = \rho\partial^2 u_i/\partial t^2 \tag{2}$$

Here u_i (i =1,2,3) are the displacement components of the obstacle points, σ_{ij} are the components of the stress tensor, ρ is the specific weight of the barrier material; by the same indices in (2) is meant summation, the comma before the index corresponds to the derivative with respect to the coordinate following the comma.

It is assumed that the layers of barrier material can be represented as an anisotropic linearly deformable body

$$\varepsilon_{ij} = A_{ijmn}\sigma_{mn} \tag{3}$$

with parameters of elastic compliance A_{ijmn} [5].

The linear connection between the displacement components u_i and the small deformations ε_{ij}

$$\varepsilon_{ij} = 0.5(u_{i,j} + u_{j,i}) \tag{4}$$

closes the system of defining equations (1) - (4) for the solution of the problem of the introduction of a spherical impactor into a deformable plate. The plate may be laminated with identical or different mechanical characteristics of the material of the individual layers.

Thus, it is necessary to find a joint solution of equations (1) - (4) under the condition that at the initial instant of time (t = 0) the obstacle is at rest, and the impactor has an initial velocity v0 in the direction of the normal to the obstacle surface.

In the formulated problem, the interaction force between the spherical impactor and the deformable obstacle F is a function of time t. In static problems about a rigid stamp [4], [6], the force F (see, equation (1)) is assumed to be given and then the contact problem is solved. In this case, the force F is one of the unknown quantities, varying as the impactor is inserted into the obstacle body.

It is convenient to study the dimensionless parameters w, τ, f, x^*_i, w_i, σ^*_{ij}, A_{ijmn}:

$$x_i = x^*_i \cdot L,\ s = w\cdot h,\ u_i = w_i\cdot h,\ t = \tau\cdot h/v_0,\ F = f\cdot m\cdot v_0^2/h = f\cdot\gamma\cdot V\cdot v_0^2/h,$$
$$\sigma_{ij} = \sigma^*_{ij}\cdot\rho\cdot(L/h)\cdot v_0^2,\ \ A_{ijmn} = A^*_{ijmn}/(\rho\cdot(L/h)\cdot v_0^2) \tag{5}$$

Here L is the characteristic length (for example, half the length of the side of the square), h is the total thickness of the multilayered barrier, γ is the specific gravity of the impactor material, and V is its volume.

With respect to the dimensionless parameters, the equations of motion of the impactor (1) and the barrier (2) take the form

$$\partial^2 w/\partial\tau^2 = f, \quad \sigma^*_{ij,j} = \partial^2 w_i/\partial\tau^2 \tag{6}$$

The form of the relationship between stresses and deformations (3) does not change if dimensional parameters are replaced by their dimensionless analogs. In the expressions for deformations (4) on the right, dimensionless quantities should be put.

Equations (6) must be solved under the initial conditions

$$w=0,\ \partial w/\partial\tau=1,\ w_i=0,\ \partial w_i/\partial\tau=0 \ \text{ for } \tau=0 \tag{7}$$

and boundary conditions

$$\begin{gathered} w_1 = w_2 = w_3 = 0 \text{ for } x^*_1 = \pm 1,\ \sigma^*_{22} = \sigma^*_{21} = \sigma^*_{23} = 0 \text{ for } x^*_2 = \pm 1 \text{ and} \\ \int_S \sigma^*_{33} ds = f,\ \sigma^*_{31} = \sigma^*_{32} = 0 \text{ for } x^*_3 = h/2L,\ \sigma^*_{33} = \sigma^*_{31} = \sigma^*_{32} = 0 \text{ for } x^*_3 = 0 \end{gathered} \tag{8}$$

Here 2L is the length of the side of the square plate, S is the variable dimensionless contact area of the striker and the barrier. For □ = 0, the contact area is S = 0.

3 SCALE PARAMETERS

Let the characteristic length L change by a factor of α and the new length $\Lambda = \alpha L$. In order that the dimensionless coordinates x^*_i do not change under these conditions, the real coordinate xi must change exactly α times ($X_i = \alpha \cdot x_i = x^*_i \cdot \alpha L = x^*_i \cdot \Lambda$).

Under the conditions (8), the equality of the force of the impactor and the resistance of the plate must be satisfied on the dimensionless surface $x^*_3 = h/2L$. It does not change if the thickness changes exactly by α times, i.e. . $x^*_3 = h/2L = \alpha h/2\Lambda = H/2\Lambda$, $H = \alpha h$. In this case, the movements of both the striker s and the barriers u_i also change exactly by a factor of α. In fact, $S = \alpha s = w\alpha h = wH$, $U_i = \alpha u_i = w_i \alpha h = w_i H$.

The time t can be written in the form $t = \tau \cdot h/v_0 = \tau \cdot H/\alpha v_0$ when the plate size is changed. If the speed of the drummer remains unchanged, then the real time should be changed exactly α times, i.e. $T = \alpha t = \tau \cdot H/v_0$. The real time can be saved. In this case, the initial velocity of the striker V_0 must be increased exactly by a factor of α, i.e. $t = \tau \cdot h/v_0 = \tau \cdot H/(\alpha v_0) = \tau \cdot H/V_0$, $V_0 = \alpha v_0$.

In accordance with (5), the dimensionless force $f = h \cdot F/(m \cdot v_0^2)$. When changing the size of the plate and the speed of the hammer becomes $f = \alpha \cdot F \cdot H/(m \cdot V_0^2)$. It can be seen that if the mass of the impactor does not change, then the acting force should change exactly by a factor of α, i.e. $f = \alpha \cdot F \cdot H/(m \cdot V_0^2) = \Phi \cdot H/(m \cdot V_0^2)$ and $\Phi = \alpha \cdot F$. If the mass of the impactor is increased exactly α times (that is, $M = \alpha m$), then the force will change by α^2 times. In fact, $f = \alpha \cdot F \cdot H/(m \cdot V_0^2) = \alpha^2 \cdot F \cdot H/(M \cdot V_0^2) = \Phi \cdot H/(m \cdot V_0^2)$ and $\Phi = \alpha^2 \cdot F$.

It is interesting to note that in the investigated single system the impactor is an obstacle calculated at the same time instant t the ratio of the increment of the kinetic energy of the impactor $T = 0.5 \cdot m \cdot v^2$ to the change in the potential deformation energy $U = 0.5 \cdot \sigma_{ij} \cdot \varepsilon_{ij}$ of the barrier is a constant value.

4 STATEMENT OF NUMERICAL EXPERIMENTS

4.1 Isotropic flat plate (metal)

Four flat square plates, the dimensions of which are given in Table 1, were considered for comparative studies. The samples were rigidly fixed at two opposite edges (they are indicated in red in Figure 1) and are free on the other two edges. The center of the plate was struck by a spherical drummer (see Figure 1). The diameter of the impactors was chosen in accordance with the dimensions of the sample. The chosen diameters of the strikers and their weights are given in Table 1. Each specimen was subjected to impact with impact velocities v1 = 150 m / s, v2 = 175 m / s and v3 = 200 m / s.

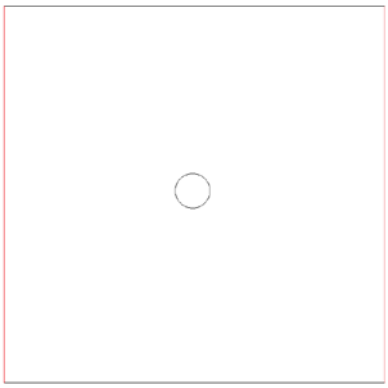

Figure 1: Scheme of fixing and loading the sample.

Table 1: Dimensions of plate and impactor

Scale factor, n	Plate dimensions, mm	Impactor diameter, mm	Impactor weight, g
¼	25x25x0,5	2,5	0,03516
½	50x50x1	5	0,2813
¾	75x75x1,5	7,5	0,9493
1	100x100x2	10	2,25

The isotropic material of the impactor was assumed to be absolutely elastic with the properties given in Table 2. The material of isotropic plates is deformed elastically and plastically according to the bilinear law. The properties of the material of the plates are given in Table 2. The ultimate deformation was specified as the criterion of failure, which is assumed to be 12% in the calculations.

Table 2: Properties of plate and impactor materials

	Plate	Impactor
Density ρ, kg / m^3	4300	4300
Young's modulus, MPa	120000	120000
Poisson's ratio, ν	0,3	0,3
Yield strength, MPa	650	-
Tangential modulus of elasticity, MPa	6000	-
Limiting deformation,%	12	-

4.2 Laminated orthotropic flat plate (composite material)

Also, comparative design studies of four flat square laminated plates of orthotropic material were carried out. The dimensions of the investigated plates are given in Table 3. In the calculations, the samples, as well as for the metal, were rigidly fixed along the two opposite edges (they are indicated in red in Figure 1) and are free at the other two edges. The center of the plate was struck by a

spherical drummer (see Figure 1). The diameter of the impactors was chosen in accordance with the dimensions of the sample. The chosen diameters of the strikers and their weights are given in Table 3. Each sample was impacted with the impact velocities v1 = 25 m / s, v2 = 35 m / s and v3 = 45 m / s.

Table 3: Dimensions of plate and impactor

Scale factor, n	Plate dimensions, mm	Impactor diameter, mm	Impactor weight, g
¼	25x25x0,25 (1 layer)	2,5	0,03516
½	50x50x0,5 (2 layers)	5	0,2813
¾	75x75x0,75 (3 layers)	7,5	0,9493
1	100x100x1 (4 layers)	10	2,25

The plate was modeled by thin-walled shells with three integration points.

The isotropic material of the impactor was assumed to be absolutely elastic with the properties given in Table 4. The material of the layer was an orthotropic material with the properties given in Table 4. The ultimate stresses were taken as the criterion for destruction. The coefficient of friction between the layers, as well as the layers and the impactor, was 0.2.

Table 4: Properties of plate and impactor materials

	Plate	Impactor
Density ρ, kg/m^3	1440	4300
Young's modulus, E_x MPa	22900	120000
Young's modulus, E_y MPa	22900	-
Poisson's ratio, ν_{xy}	0,3	0,3
Shear modulus, G_{xy} MPa	280	-
Shear modulus, G_{xz} MPa	350	-
Shear modulus, G_{yz} MPa a	350	-
Strength in the x-direction, MPa	520	-
Strength in the y-axis, MPa	520	-

4.3 Laminated orthotropic model of fan case (composite material)

Four models of fan case, the dimensions of which are given in Table 5, were considered for comparative studies. The hull was modeled by 3 thin-walled shells, the first of which was rigidly fastened to one of the ends, the other two layers were absolutely free and were connected only by frictional forces. The impact was produced by the imitator of the blade, which was a regular truncated pyramid (Figure 2), the dimensions of which are given in Table 5. The circumferential velocity for various sizes was chosen on the basis of equality of velocity at the periphery of the blade simulator for all types of size.

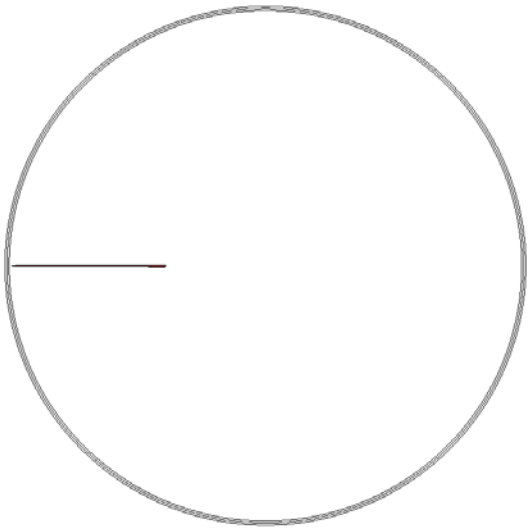

Figure 2: Model of fan case with the imitator of the blade.

Table 5: Dimensions of the model of fan case and imitator of the blade

Scale factor, n	Model of fan case			Imitator of the blade			
	Ø, mm	l, mm	t, mm	L, mm	h, mm	t, mm	ω, 1/rad
¼	500	150	2x3=6	150	50	1-2	1680
½	1000	300	4x3=12	300	100	2-4	840
¾	1500	450	6x3=18	450	150	3-6	560
1	2000	600	8x3=24	600	200	4-8	420

The isotropic material of the impactor was assumed to be elastic - plastic with a bilinear law (see Table 6). As a criterion for destruction of the blade simulator, the limiting deformation was set, which in the calculations was assumed to be 12%. The layer material was an orthotropic material with the properties given in Table 6. The coefficient of friction between the layers, as well as the layers and the impactor, was 0.2.

Table 6: Properties of model of fan case and imitator of blade materials

	Model of fan case	Imitator of blade
Density ρ, kg/m^3	1440	4300
Young's modulus, E_x MPa	22900	120000
Young's modulus, E_y MPa	22900	-
Poisson's ratio, ν_{xy}	0,03	0,3
Shear modulus, G_{xy} MPa	280	-
Shear modulus, G_{xz} MPa	350	-
Shear modulus, G_{yz} MPa a	350	-
Strength in the x-direction, MPa	520	-
Strength in the y-axis, MPa	520	-
Yield strength, MPa	-	650
Tangential modulus of elasticity, MPa	-	6000
Limiting deformation,%	-	12

5 RESULTS AND DISCUSSION

5.1 Isotropic flat plate (metal)

In Figure 4a shows a typical plot of the force F acting on the impactor from the displacement Δ of the impactor for four plates with scaling factors n at the impact energy T_2 = 34,46n^3 Дж (v_2=175 м/с). The impact force F was determined from equation (9)

$$F = ma\,, \tag{9}$$

where m is the mass of the striker, and a is the acceleration of the impactor.

The acceleration *a* at each instant of time t was found from the calculated curve of the dependence of the velocity V (see Figure 3) on the time t according to the following equation

$$a = -\frac{V_{i+1} - V_i}{t_{i+1} - t_i} \tag{10}$$

where V is the velocity of the striker, t is the time.

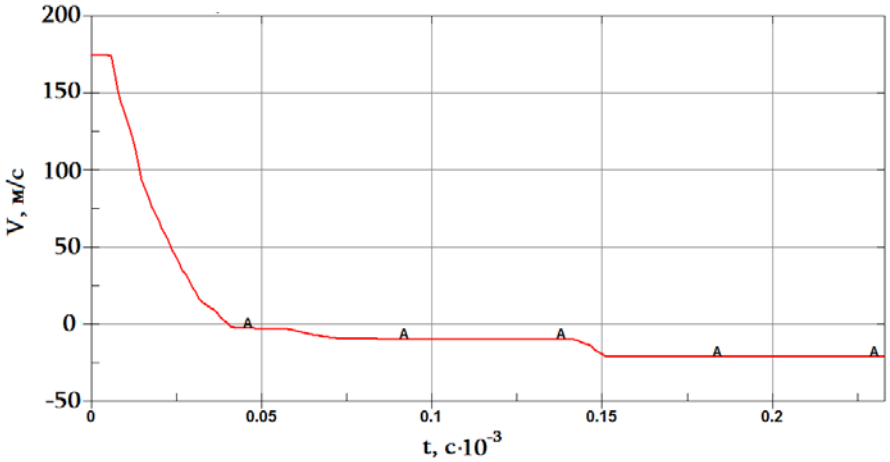

Figure 3: Typical graph of velocity versus time.

To level the scale factor, scale factors for the force F and displacement Δ were chosen. For the force F, the chosen scale factor was - 1/n^2, and for the displacement Δ it turned out to be equal to 1/n. Below in Figure 4b is a graph of the dependence of the force F on the displacement Δ, taking into account the selected scale factors.

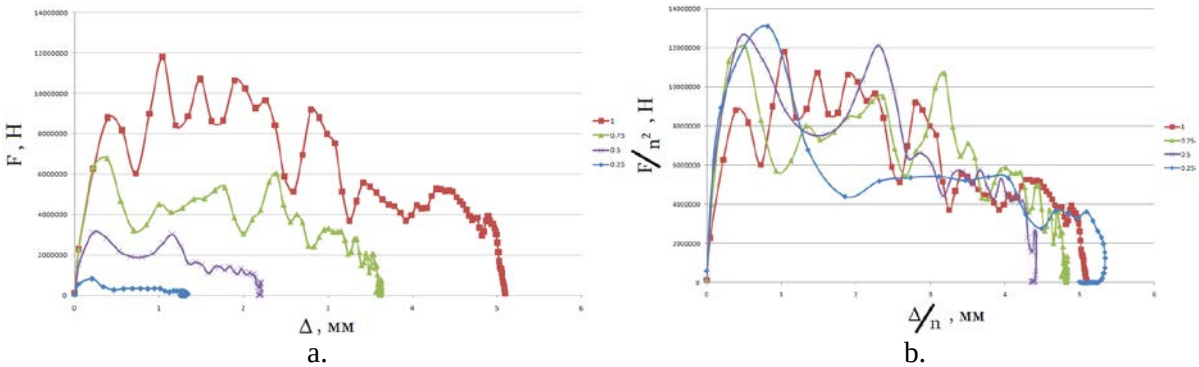

a. b.

Figure 4: a – Graph of the dependence of the force F on the displacement Δ; b – Graph of the dependence of the "normalized" force F on the "normalized" displacement Δ.

It can be seen from Figure 4b that the graphs of the dependence of the "normalized" force F on the "normalized" displacement Δ are similar in appearance for all four types of plates, taking into account scale factors. The adopted scaling factors are consistent with other works (see, for example, [2]).

By the trapezium method, the area S was calculated under each curve of the force F versus the displacement Δ of the impactor for the four types of plates shown in Figure 4. The calculated areas S are given in Table 6. They correspond to the work U performed by the impactor when the plate is deformed. The work U, multiplied by n^{-3}, corresponds to the "normalized" area S/n^3 (see Table 6) under the curves of the dependence of the "normalized" force F on the "normalized" displacement Δ, shown in Figure 5. From Table 6 it can be seen that the errors in the values of the normalized areas S/n^3 for samples of different sizes are sufficiently small. This circumstance makes it possible to take the work $U=S/n^3$ as the parameter of reduction to a single scale in the study of the impact resistance of samples.

Table 6: Results for a flat isotropic plate

n	v_1=150 m/s,			v_2=175 m/s			v_3=200 m/s		
	S	S/n^3	$\Delta S/n^3$,%	S	S/n^3	$\Delta S/n^3$,%	S	S/n^3	$\Delta S/n^3$,%
1/4	$3{,}90\cdot10^5$	$2{,}50\cdot10^7$	1,34	$5{,}03\cdot10^5$	$3{,}22\cdot10^7$	6,1 %	$7{,}02\cdot10^5$	$4{,}49\cdot10^7$	0,51
1/2	$3{,}16\cdot10^6$	$2{,}53\cdot10^7$	0	$4{,}21\cdot10^6$	$3{,}37\cdot10^7$	1,8 %	$5{,}62\cdot10^6$	$4{,}50\cdot10^7$	0,58
3/4	$1{,}07\cdot10^7$	$2{,}54\cdot10^7$	0,25	$1{,}44\cdot10^7$	$3{,}41\cdot10^7$	0,5 %	$1{,}89\cdot10^7$	$4{,}48\cdot10^7$	0,23
1	$2{,}53\cdot10^7$	$2{,}53\cdot10^7$	0	$3{,}43\cdot10^7$	$3{,}43\cdot10^7$	0 %	$4{,}47\cdot10^7$	$4{,}47\cdot10^7$	0

The nature of the deformation of samples of different sizes upon impact with one velocity (v_1=150 m/s, v_2=175 m/s, v_3=200 m/s), but with energies proportional to n^3 is practically the same. This is evident from Figure 5. In Figure 5b shows the cross sections of the plates (n=1/4,1/2,3/4,1) after impact with velocity v_2 = 175 m/s, energy $T_2 = 34{,}46n^3$ J. As can be seen from Figure 5, the level of plastic deformations almost the same for all four sizes.

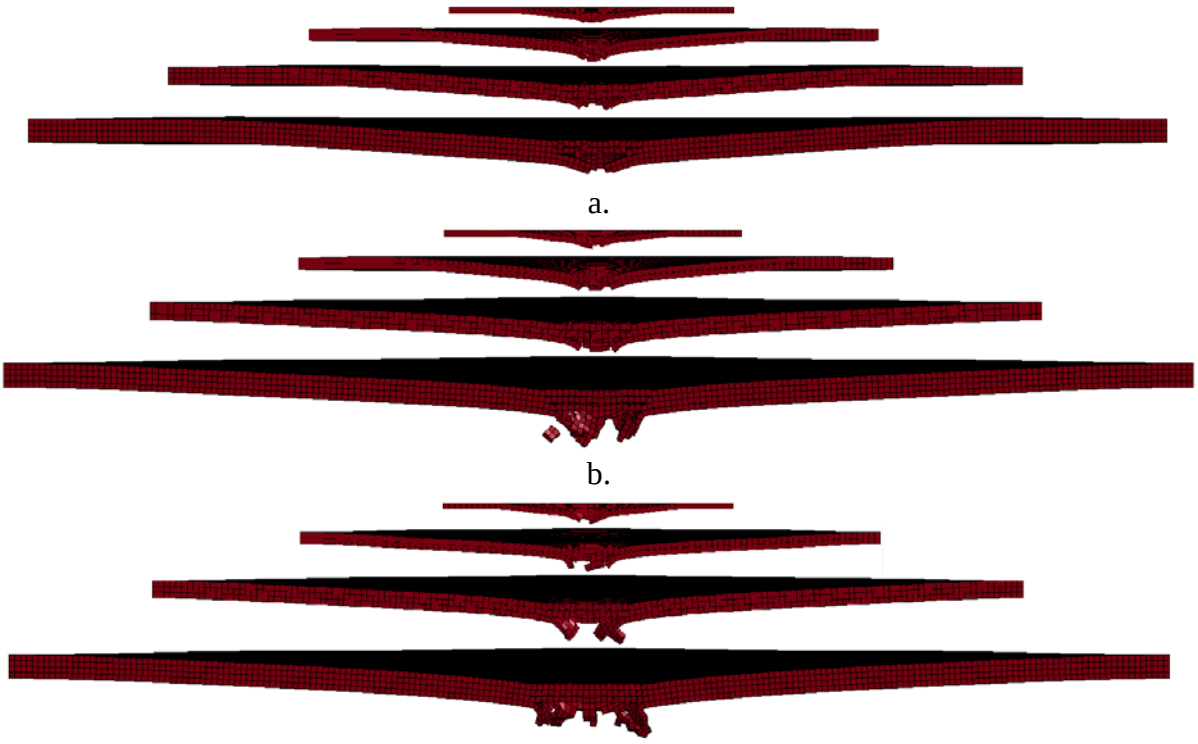

a.

b.

c.

Figure 5: Cross sections of samples of different sizes after impact with velocities v_1 = 150 m/s – a, v_2 = 175 m/s – b., v_3 = 200 m/s – c.

The curves in Figure 5, the results on the nature of the deformation of the samples draw attention to the fact that the dependences of the relative displacements of Δ/h samples of different sizes for the same "normalized" impact energy are approximately the same, but can vary from one speed v to another. As a result, the dependences of the dimensionless displacement Δ on the dimensionless energy χ were constructed for three points corresponding to three velocities (v_1=150 m/s, v_2=175 m/s, v_3=200 m/s), which were calculated using the following formulas:

$$\delta = \frac{\Delta}{h} \tag{11}$$

$$\chi = \frac{E_k}{E\delta_{np}d^3} \tag{12}$$

where Δ is the displacement of the impactor, h is the plate thickness, E_k is the initial kinetic energy of the impactor, E is the modulus of elasticity of the plate material, δ_{cr} is the ultimate deformation, and d is the diameter of the impcator.

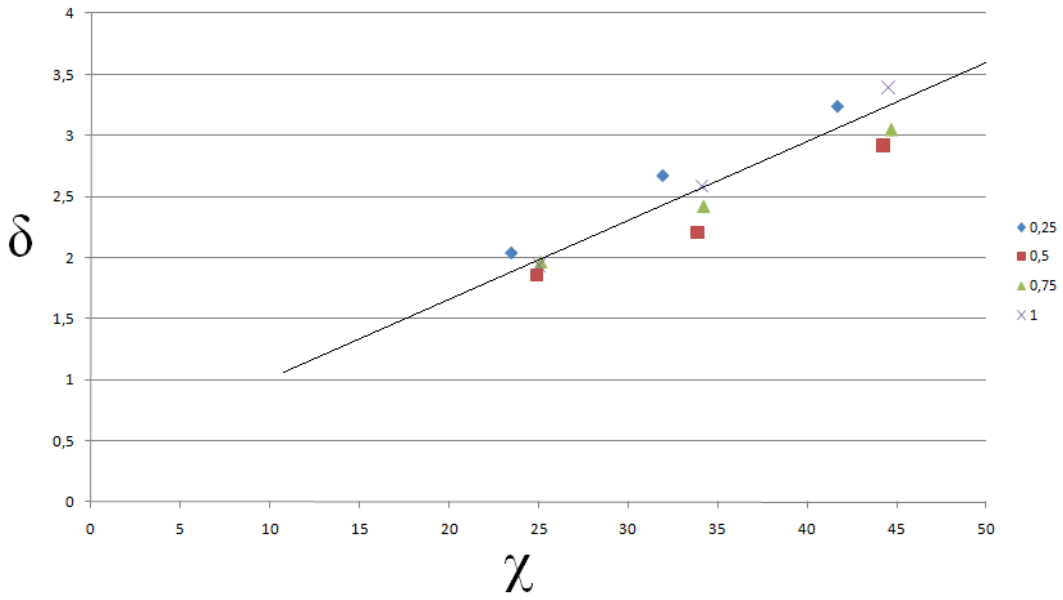

Figure 6 – Dependence of the dimensionless displacement Δ on the dimensionless energy χ.

As can be seen from Figure 6 the dependence of the dimensionless displacement Δ on the dimensionless energy χ, despite the fact that deformation of the barrier is nonlinear, it is practically linear. Thus, it was shown that the fracture forms and failure mechanisms were similar in all four scale sizes of the samples studied at the corresponding impact rates. This circumstance, in spite of small deviations, allows, by extrapolation, to switch to any level of energies, including the energy levels that occur when a real blade breaks off and moves the real fan case.

5.2 Laminated orthotropic flat plate (composite material)

For a layered orthotropic plate, a plot of the force F versus the displacement Δ (Figure 7a) and a plot of the dependence of the "normalized" force F on the "normalized" displacement Δ (Figure 7b) were also plotted.

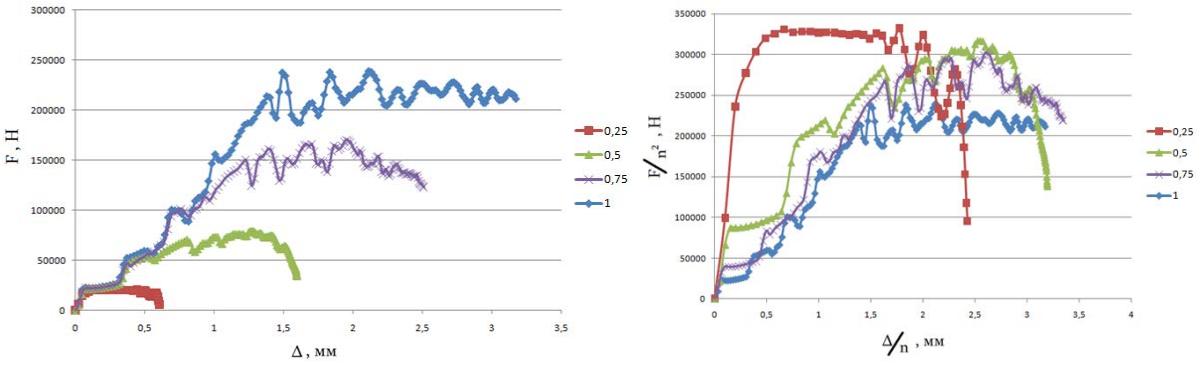

a. b.

Figure 7: a – The graph of the dependence of the force F on the displacement Δ; b – Graph of the dependence of the "normalized" force F on the "normalized" displacement Δ.

Just as for a isotropic body, the area S was calculated under each curve of the dependence of the force F on the displacement Δ of the impactor for the four types of plates shown in Figure 7.

Table 7: Results for a flat laminated orthotropic plate

n	v_1=25 m/s,			V_2=35 m/s			v_3=45 m/s		
	S	S/n^3	$\Delta S/n^3$,%	S	S/n^3	$\Delta S/n^3$,%	S	S/n^3	$\Delta S/n^3$,%
1/4	$1{,}08\cdot10^4$	$6{,}91\cdot10^5$	8,85	$2{,}15\cdot10^4$	$1{,}38\cdot10^6$	10,9	$3{,}21\cdot10^4$	$2{,}05\cdot10^6$	7,0
1/2	$8{,}34\cdot10^4$	$6{,}74\cdot10^5$	6,2	$1{,}72\cdot10^5$	$1{,}38\cdot10^6$	10,9	$2{,}52\cdot10^5$	$2{,}02\cdot10^6$	5,0
3/4	$2{,}80\cdot10^5$	$6{,}64\cdot10^5$	4,52	$5{,}68\cdot10^5$	$1{,}35\cdot10^6$	8,6	$8{,}20\cdot10^5$	$1{,}94\cdot10^6$	1,3
1	$6{,}35\cdot10^5$	$6{,}35\cdot10^5$	0	$1{,}24\cdot10^6$	$1{,}24\cdot10^6$	0	$1{,}92\cdot10^6$	$1{,}92\cdot10^6$	0

The forms of failure and the mechanisms of destruction were similar in all four large-scale dimensions of the samples studied at the corresponding impact rates.

5.3 Laminated orthotropic model of fan case (composite material)

In Figures 8a and 9a show typical plots of the kinetic energy of the blade imitator and the potential energy of the model of fan case versus time. To level the scale factor, scaling coefficients were calculated for the kinetic energy of the imitator of the blade E_k, the potential energy of the body model E_p and the time t. For the kinetic energy of the imitator of the blade E_k and the potential energy of the model of the fan case E_p the scaled scale factor was - $1/n^3$, and for the time t it turned out to be 1/n. Below in Figures 8b and 9b are graphs of the dependence of the kinetic energy E_k and the potential energy E_p on the time t, taking into account the selected scaling factors.

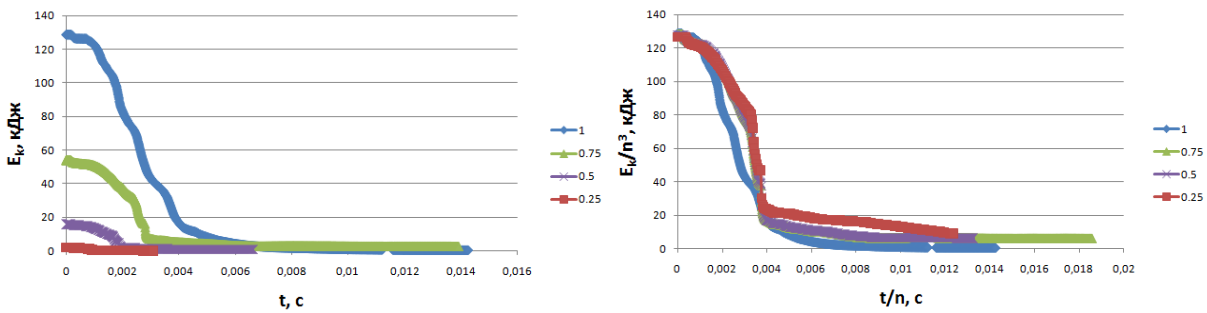

a. b.

Figure 8: a – Graph of dependence of the kinetic energy of the imitator of the blade E_k on the time t; b – The graph of the dependence of the "normalized" kinetic energy of the imitator of the blade E_k on the "normalized" time t.

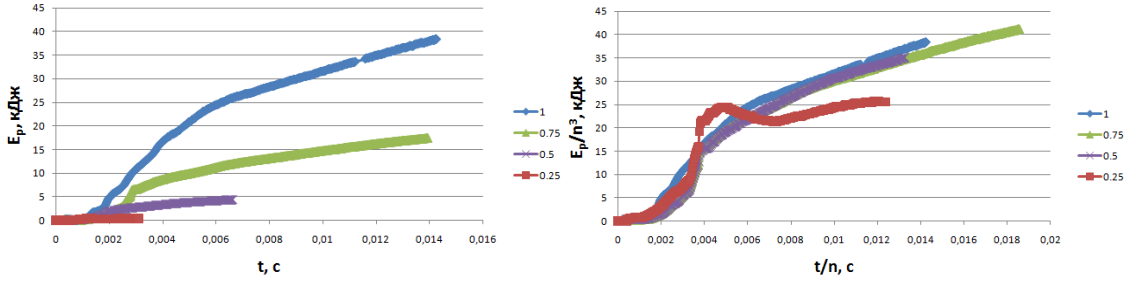

a. b.

Figure 9:a – Graph of dependence of the potential energy of the model of the fan case E_p on the time t; b – The graph of the dependence of the "normalized" potential energy of the model of the fan case E_p on the "normalized" time t.

From Figures 8b and 9b it can be seen that the graphs of the dependence of the "normalized" kinetic energy of the blade imitator E_k and the "normalized" potential energy of the model of the fan case E_p from the "normalized" time t are similar for all four types of shell model sizes with scale factors.

Also, plots of the potential energy dependence for each shell of the model of the fan casewere constructed (Figures 10-12).

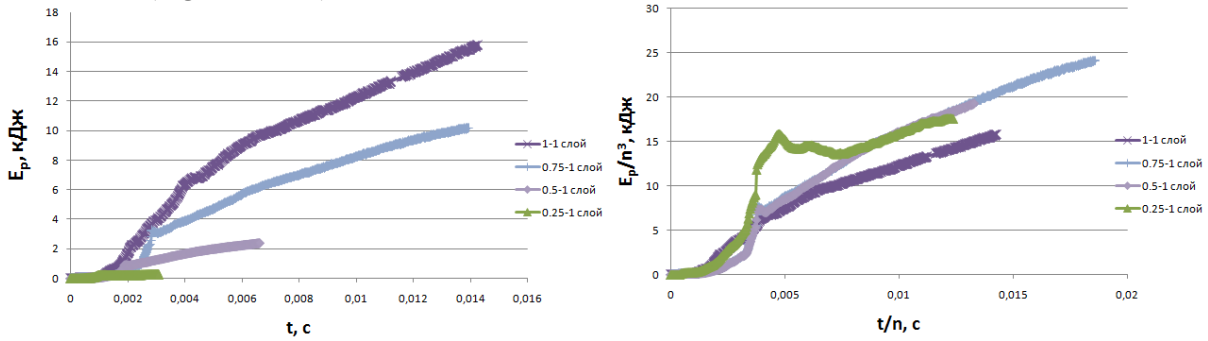

a. b.

Figure 10: a – Graph of the dependence of the potential energy of the 1st layer of the model of the fan case E_p on the time t; b – Graph of the dependence of the "normalized" potential energy of the 1st layer of the model of the fan case E_p from the "normalized" time t.

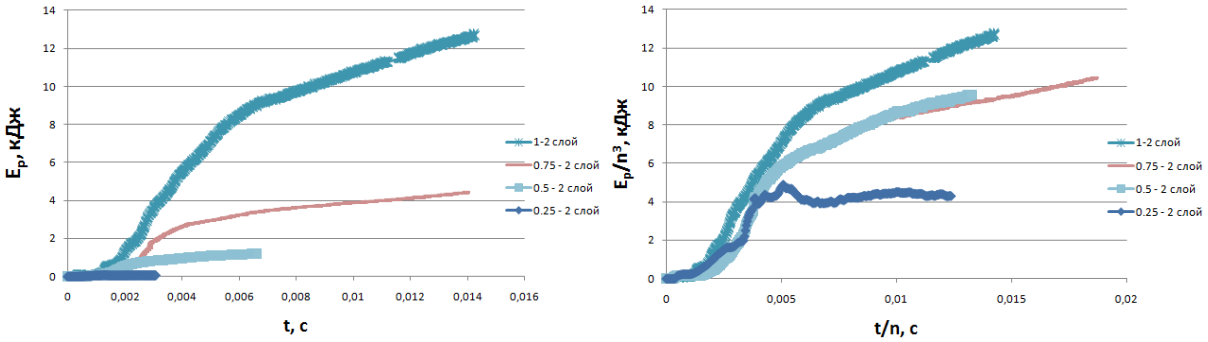

a. b.

Figure 11: a – Graph of the dependence of the potential energy of the 2nd layer of the model of the fan case E_p on the time t; b – Graph of the dependence of the "normalized" potential energy of the 2nd layer of the model of the fan case E_p from the "normalized" time t.

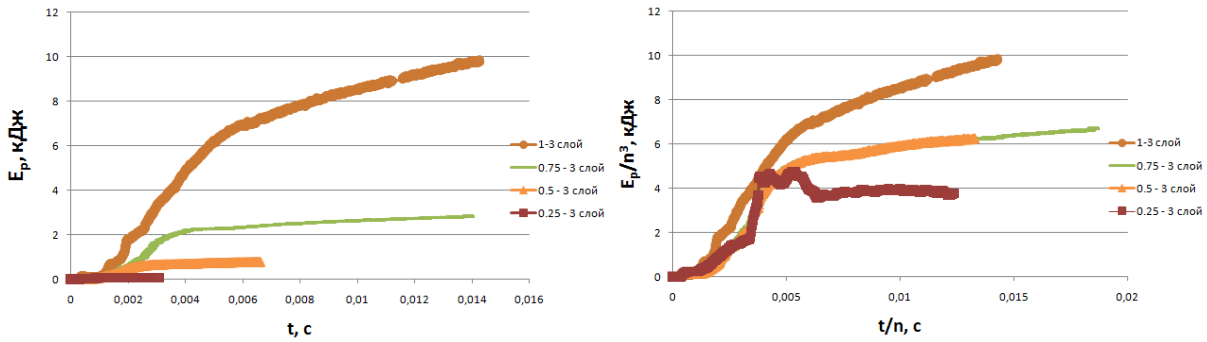

a. b.

Figure 12: a – Graph of the dependence of the potential energy of the 3rd layer of the model of the fan case E_p on the time t; b – Graph of the dependence of the "normalized" potential energy of the 3rd layer of the model of the fan case E_p from the "normalized" time t.

As can be seen from these graphs, the potential energy of individual layers differs for different scale factors, while the potential energy of the entire model of fan case is practically the same for all scale factors (the largest deviation is the graph for the scale factor 0.25).

5 CONLUSIONS AND OUTLOOK

The performed researches establish the parameters that allow to start developing the basics of similarity models in problems of ensuring safety in the destruction of fan blades of advanced turbojet engines.

REFERENCES

[1] Sedov L.I. -Methods of similarity and dimension in mechanics – The Main Publishing house "Science", Moscow, 1977, 439 p.

[2] N. Jones – Some comments on the scaling of inelastic structures loaded dynamically– Impact Research Centre. Department of Mechanical Engineering. The University of Liverpool. Liverpool. United Kingdom

[3] J. G. Carrillo1, S. McKown1, M. Mujib1 and W. J. Cantwell1. R. Day – Scaling effects in the velocity impact response of fibre metal laminates

[4] L.S. Leibenson - Course of the theory of elasticity - OGIZ-Gostekhizdat, 1947,464 p.

[5] S.G. Lekhnitsky - Theory of elasticity of an anisotropic body - Science Publishers, Moscow, 1977, 416 p.

[6] L.A. Galin - Contact problems of the theory of elasticity and viscoelasticity - Science Publishers, Moscow, 1980, 304 p.